

# We are IntechOpen, the world's leading publisher of Open Access books Built by scientists, for scientists

6,900

Open access books available

186,000

International authors and editors

200M

Downloads

Our authors are among the

154

Countries delivered to

TOP 1%

most cited scientists

12.2%

Contributors from top 500 universities



WEB OF SCIENCE™

Selection of our books indexed in the Book Citation Index  
in Web of Science™ Core Collection (BKCI)

Interested in publishing with us?  
Contact [book.department@intechopen.com](mailto:book.department@intechopen.com)

Numbers displayed above are based on latest data collected.  
For more information visit [www.intechopen.com](http://www.intechopen.com)



## Dynamic Analysis of a DC-DC Multiplier Converter

J. C. Mayo-Maldonado, R. Salas-Cabrera, J. C. Rosas-Caro,  
H. Cisneros-Villegas, M. Gomez-Garcia, E. N. Salas-Cabrera,  
R. Castillo-Gutierrez and O. Ruiz-Martinez  
*Instituto Tecnológico de Ciudad Madero  
Ciudad Madero, Mexico*

### 1. Introduction

Renewable energy generation systems bring the promise of providing green energy which is highly desirable for decreasing global warming. Therefore, renewable energy systems are gaining attention among researchers.

In terms of power electronics, several challenges are emerging with the advent of the green energy generation systems. The first issue is that renewable energy power sources such as Photo-Voltaic PV panels, fuel cells and some wind turbine generators provide a low level dc voltage. This voltage must be boosted and then inverted in order to be connected to the grid. Since the level of the output voltage of these power sources depends on the weather conditions, there should be a method to control the generated voltage.

Other types of green energy power sources such as AC machine based wind generators provide a low level ac voltage with amplitude and frequency depending on the wind speed. A common method to deal with the generated ac voltage is to rectify it, then a DC-DC converter is used to boost it. Once the boosted DC voltage is controlled, it may feed an electric load under some operating range or it may be inverted for connecting it to the grid.

This is a scenario of increased interest in DC-DC converters with high conversion ratios. Several converters have been proposed R. D. Middlebrook (1988), D. Maksimovic et al. (1991), B. Axelrod et al. (2008), Zhou Dongyan (1999), Leyva-Ramos J (et al 2009), however all of them are complex compared with conventional single-switch converters. Some desirable features of those converters are a high conversion ratio without the use of extreme duty cycles and a transformer-less topology that allows the use of high switching frequency providing high efficiency.

One of the recently proposed converters is the multiplier boost converter (MBC) which is also known as multilevel boost converter Rosas-Caro J.C. et al (2010), Rosas-Caro J.C. et al (2008), Rosas-Caro J.C. et al (2008), Mayo-Maldonado J.C. et al (2010). This topology combines the traditional single-switch boost converter with a Cockcroft-Walton voltage multiplier. Fig. 1 shows the  $N_x$  DC-DC Multiplier Boost Converter ( $N_x$  MBC). The nomenclature  $N_x$  is associated with the number of capacitors at the output of the converter. The main advantages of the MBC are (i) high voltage gain without the use of extreme duty cycles and transformer-less, (ii) self balancing, in other words the multiplier converter maintains the

voltage of the capacitors at the output equal to each other, (iii) the structure is very simple and only one switch is required.

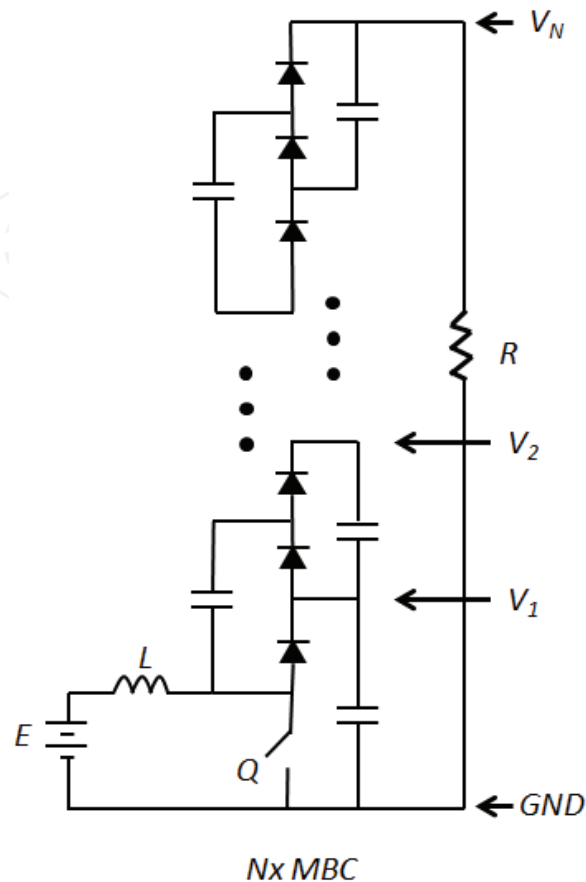


Fig. 1. Electrical diagram of the Nx Multiplier Boost Converter.

There are several contributions in this paper. Since the MBC is a recently proposed topology its dynamic behavior has not been studied deeply. We propose both a full order nonlinear dynamic model and a reduced order nonlinear dynamic model for the MBC. In addition, a new controller for the MBC is obtained by utilizing the differential geometry theory, A. Isidori (1995). In particular, input-output feedback linearization is employed to control the inductor current. In our approach, the output voltage is indirectly controlled by defining a reference for the inductor current. The controller is derived by using the proposed reduced order model. The stability of the zero dynamics of the closed loop system is analyzed. Experimental results of the closed loop implementation are also presented.

Previous works present different models for other boost converters. In Morales-Saldana J.A. et al (2007), authors propose both nonlinear and average linear models for a quadratic boost converter. In Bo Yin et al. (2009), authors propose a single-input-single-output model for an AC-DC boost converter; the model is similar to the model of the conventional DC-DC boost converter.

Different control techniques for power electronics devices can be found in the literature. In Hebertt Sira-Ramirez et al. (2006), a wide series of control techniques are presented for well known power electronics converters, including the conventional DC-DC boost converter. In Leyva-Ramos J (et al 2009), authors present experimental results of the implementation of a

current-mode control for the quadratic boost converter. In Gensior A. et al. (2009), authors present some current controllers for three-phase boost rectifiers.

## 2. Modeling of the DC-DC Multiplier Boost Converter

In this section we will be presenting both the full order nonlinear dynamic model and a reduced order nonlinear dynamic model for the MBC. The proposed models are obtained from the equivalent circuits depending on the commutation states of the converter. The derived reduced order model is able to define an approximate dynamics for the MBC containing any number of levels without modifying the order of the dynamic model. This feature provides several advantages for control design and implementation.

### 2.1 Full order modeling

Let us consider the electrical diagram in Fig. 2 that depicts a 2x MBC. This converter has 2 capacitors at the output ( $C_1$  and  $C_2$ ). For this particular converter the number  $N$  is equal to 2. In this section  $V_3$  is a notation related to a voltage across a capacitor that is not at the output of the MBC. In addition, let us define an input  $u = \{1,0\}$  associated with the commutation states of the switch.

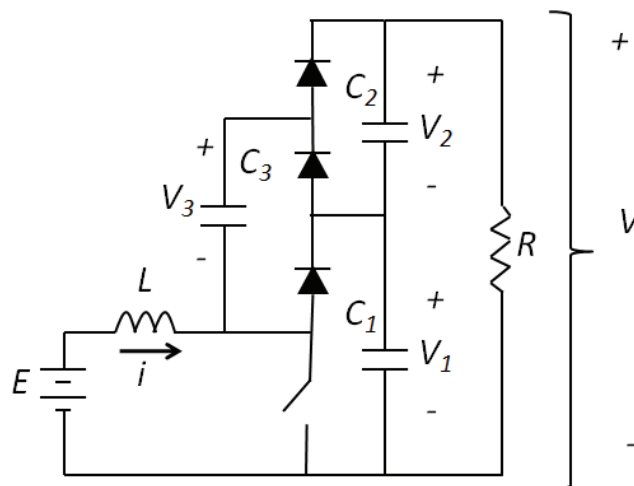


Fig. 2. Electrical diagram for a 2x DC-DC Multiplier Boost Converter.

Figure 3 shows the equivalent circuit for a 2x MBC when the switch is closed, this is  $u = 1$ . Equations (1)-(4) represent the dynamics related to the inductor and the  $N + 1$  capacitors of a 2x MBC when the switch is closed.

$$\frac{d}{dt}i = \frac{1}{L}E \tag{1}$$

$$\frac{d}{dt}V_1 = -\frac{1}{(C_1 + C_3)R}V_1 - \frac{1}{(C_1 + C_3)R}V_2 - \lambda_1(t) \tag{2}$$

$$\frac{d}{dt}V_2 = -\frac{1}{C_2R}V_1 - \frac{1}{C_2R}V_2 \tag{3}$$

$$\frac{d}{dt}V_3 = -\frac{1}{(C_1 + C_3)R}V_1 - \frac{1}{(C_1 + C_3)R}V_2 + \lambda_1(t) \tag{4}$$

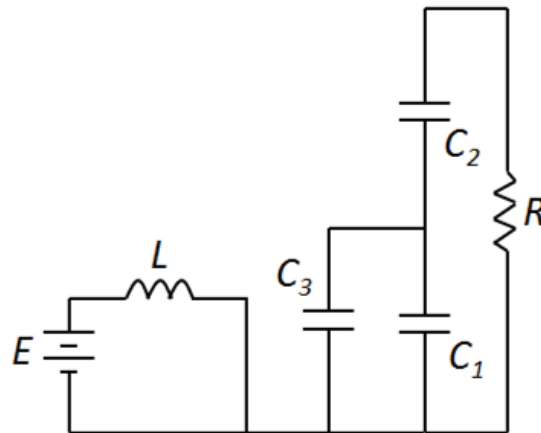


Fig. 3. Equivalent circuit for a 2x DC-DC Multiplier Boost Converter when the switch is closed.

In equation (2) and (4), function  $\lambda_1(t)$  represents a very fast transient that occurs when capacitors  $C_1$  and  $C_3$  are connected in parallel (see Fig. 3). Function  $\lambda_1(t)$  is given by the following equation

$$\lambda_1(t) = \frac{V_1 - V_3}{R_G C_1}$$

where  $R_G$  is a very small resistance. If it is assumed that the resistances of the diodes and capacitors are neglected then the value of  $R_G$  tends to be zero.

As voltages across capacitors  $C_1$  and  $C_3$  tend to be equal, the function  $\lambda_1(t)$  approximates to zero. Therefore,  $\lambda_1(t)$  defines the dynamics in which  $C_3$  obtains energy from  $C_1$  when the switch is closed. The rest of the terms of the state equations (1)-(4) produce slower transients. Figure 4 shows the equivalent circuit when the switch is opened, this is  $u = 0$ .

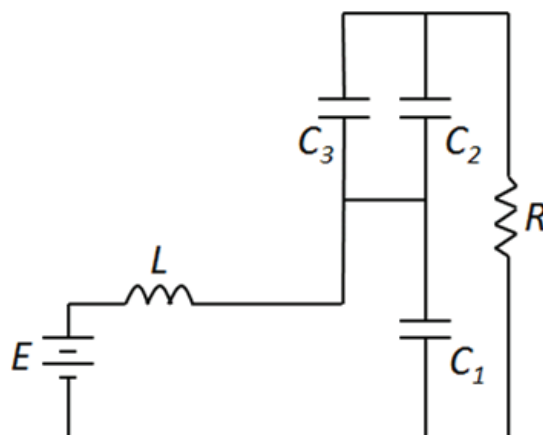


Fig. 4. Equivalent circuit for a 2x DC-DC Multiplier Boost Converter when the switch is opened.

Equations (5)-(8) represent the dynamics of the converter when the switch is opened.

$$\frac{d}{dt}i = -\frac{V_1}{L} + \frac{1}{L}E \quad (5)$$

$$\frac{d}{dt}V_1 = \frac{i}{C_1} - \frac{1}{C_1R}V_1 - \frac{1}{C_1R}V_2 \quad (6)$$

$$\frac{d}{dt}V_2 = -\frac{1}{(C_1 + C_2)R}V_1 - \frac{1}{(C_1 + C_2)R}V_2 + \lambda_2(t) \quad (7)$$

$$\frac{d}{dt}V_3 = -\frac{1}{(C_1 + C_3)R}V_1 - \frac{1}{(C_1 + C_3)R}V_2 - \lambda_2(t) \quad (8)$$

State equations associated with the voltages across capacitors  $C_2$  and  $C_3$  have a term denoted by  $\lambda_2(t)$ . This function defines a transient similar to the one defined by  $\lambda_1(t)$  when capacitors  $C_1$  and  $C_3$  were connected in parallel. The function  $\lambda_2(t)$  can be expressed as

$$\lambda_2(t) = \frac{V_3 - V_2}{R_C C_3}$$

Therefore, when the switch is closed,  $C_3$  obtains energy from  $C_1$ , this task is represented by  $\lambda_1(t)$ . On the other hand, when the switch is opened,  $C_3$  transfers energy to  $C_2$ , this is represented by  $\lambda_2(t)$ . It is possible to conclude that capacitor  $C_3$  works as the circuital vehicle that transports energy from capacitor  $C_1$  to capacitor  $C_2$ . In general, there are always  $N - 1$  capacitors transferring energy to the capacitors at the output. Let us consider the inductor current as the output of the dynamic system, this is

$$h(x) = [1 \ 0 \ 0 \ 0] [i \ V_1 \ V_2 \ V_3]^T = i \quad (9)$$

The selection of this variable as an output will be explained as the controller is derived in Section 3. The full order nonlinear dynamic model is composed by state equations (1)-(8) and the output equation in (9). When more levels are added to the circuit (see Fig. 1), the number of equations increases as well, however the system has always the same circuital structure. It is clear that the dimension of the state space increases when more capacitors are added. However, it is possible to make use of the voltage balancing feature of the MBC and obtain a reduced order model. This model should be able to approximate the dynamics of the system having any number of levels..

## 2.2 Reduced order modeling

For the purpose of reducing the order of the system, let us consider Fig. 5 and Fig.6 They depict the equivalent circuits for a 2x MBC when  $u = 1$ , and  $u = 0$ . They correspond to Fig. 3 and Fig. 4, respectively.

By employing basic principles and setting  $C = C_1 = C_2 = C_3$ , the equivalent capacitors become  $C_{eq1} = 2C$  and  $C_{eq2} = C$ . In addition, the voltage across each capacitor at the output will be considered as the output voltage divided by the number of levels at the output ( $V/N$ ). This assumption is supported by the voltage balancing feature of the MBC which was firstly presented in Rosas-Caro J.C. et al (2008). In Mayo-Maldonado J.C. et al (2010), an example of the dynamic traces of the capacitors at the output is presented. In terms of equations we have

$$V_1 \cong V_2 \cong \frac{V}{2} \quad (10)$$

where  $V$  denotes the output voltage. If there is any number of levels we may write

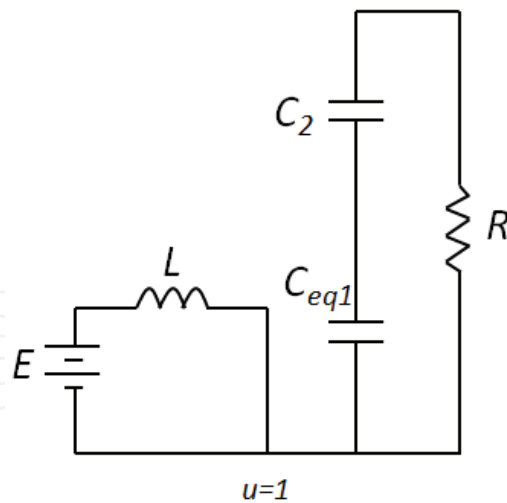


Fig. 5. Equivalent Circuit with  $u=1$  and equivalent capacitances for the 2x MBC.

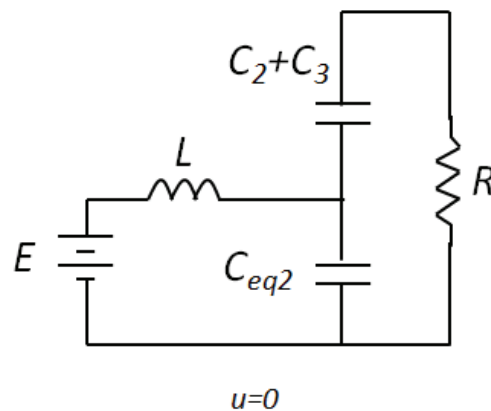


Fig. 6. Equivalent Circuit with  $u=0$  and equivalent capacitances for the 2x MBC.

$$V_1 \cong V_2 \cong V_3 \cong \dots \cong V_N \cong \frac{V}{N} \quad (11)$$

Employing the equivalent circuit shown in Fig. 5 and using equation (11) the dynamics for inductor current and the output voltage can be written as

$$L \frac{d}{dt} i = E \quad (12)$$

$$C_{eq1} \frac{d}{dt} V = -\frac{N}{R} V \quad (13)$$

It is clear that expressions (12)-(13) are valid when the switch is closed. On the other hand, based on the equivalent circuit in Fig. 6 and using equation (11), the dynamics of the system is defined as

$$L \frac{d}{dt} i = -\frac{V}{N} + E \quad (14)$$

$$C_{eq2} \frac{d}{dt} V = i - \frac{N}{R} V \quad (15)$$

Equations (14)-(15) are valid when the switch is opened. Expressions (12)-(15) may be written into a more compact form that is valid for both commutation states  $u = \{1, 0\}$ . This is

$$L \frac{d}{dt} i = -(1-u) \frac{V}{N} + E \quad (16)$$

$$[C_{eq1}u + (1-u)C_{eq2}] \frac{d}{dt} V = (1-u)i - \frac{N}{R} V \quad (17)$$

Average models are frequently employed for defining average feedback control laws in power electronics converters, Hebertt Sira-Ramirez et al. (2006). These models represent average currents and voltages. From equations (16) and (17) and considering  $u_{av}$  as the average input, we may write

$$L \frac{d}{dt} i = -(1-u_{av}) \frac{V}{N} + E \quad (18)$$

$$[C_{eq1}u_{av} + (1-u_{av})C_{eq2}] \frac{d}{dt} V = (1-u_{av})i - \frac{N}{R} V \quad (19)$$

where the average input denoted by  $u_{av}$  is actually the duty cycle of the switch. Let us denote the inductor current  $i$  as  $x_1$ , the output voltage  $V$  as  $x_2$  and  $C_{eq1}u_{av} + (1-u_{av})C_{eq2}$  as  $C(t)$ . This capacitance denoted by  $C(t)$  may be considered as a time-varying parameter. Equations (18) and (19) now become

$$L \frac{d}{dt} x_1 = -\frac{x_2}{N} + \frac{x_2}{N} u_{av} + E \quad (20)$$

$$C(t) \frac{d}{dt} x_2 = x_1 - x_1 u_{av} - \frac{N x_2}{R} \quad (21)$$

Using equations (20) and (21) and employing the inductor current as the output to be controlled, the reduced order nonlinear dynamic model for the MBC may be expressed as

$$\begin{aligned} \frac{d}{dt} x &= f(x) + g(x)u_{av} \\ y &= h(x) \end{aligned} \quad (22)$$

where

$$f(x) = \begin{bmatrix} -\frac{x_2}{NL} + \frac{E}{L} \\ \frac{x_1}{C(t)} - \frac{N x_2}{RC(t)} \end{bmatrix}; g(x) = \begin{bmatrix} \frac{x_2}{NL} \\ -\frac{x_1}{C(t)} \end{bmatrix}$$

$$h(x) = x_1; x = [x_1 \ x_2]^T$$

Equation (22) represents the reduced order average nonlinear dynamic model for the Nx MBC containing an arbitrary number of levels. Figures 7 and 8 show the comparison between the full order model and the reduced order model. These simulations are performed for the 2x MBC. The simulation of the full order model is carried out using the Synopsys Saber software and employing the electrical diagram of the 2x MBC, while the simulation of the reduced order model is obtained by using the MATLAB software to solve equation (22). The parameters involved in this simulation are  $L = 250 \mu\text{H}$ ,  $C = C_1 = C_2 = C_3 = 220 \mu\text{F}$ ,  $N = 2$ ,  $E = 40$  volts,  $R = 50 \Omega$ , and  $u_{av} = 0.6$ .

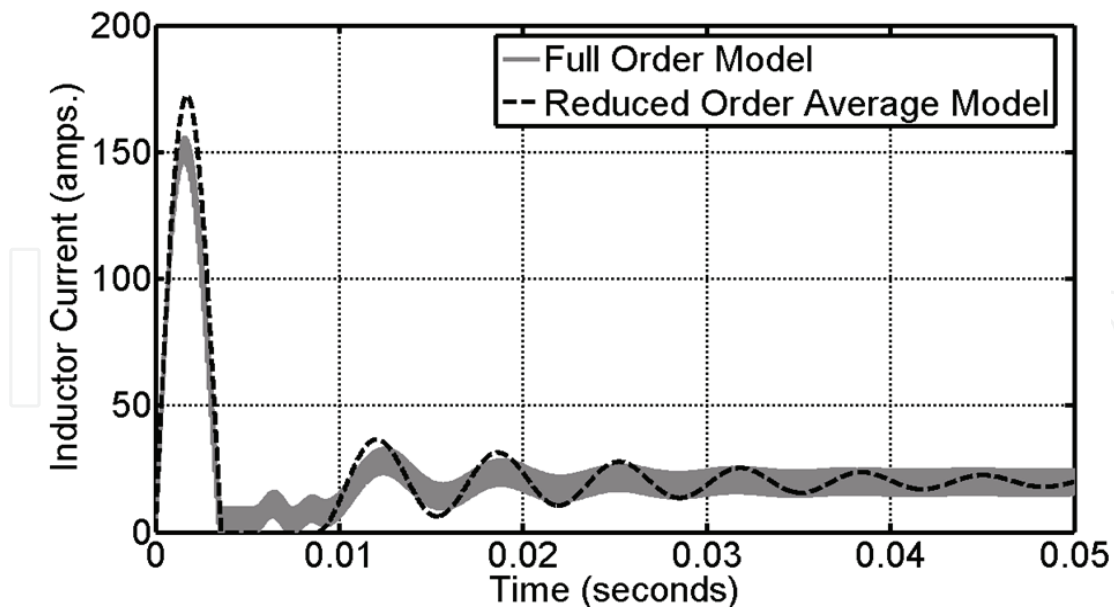


Fig. 7. Comparison between the reduced order average model and the full order model for the 2x MBC.

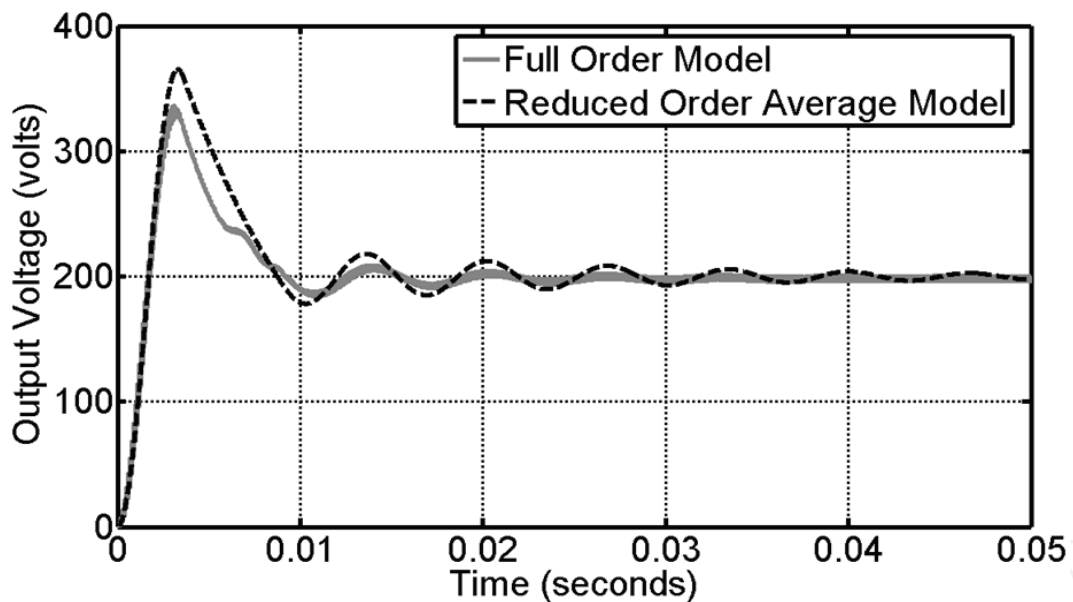


Fig. 8. Comparison between the reduced order average model and the full order model for the 2x MBC.

### 3. Control law

In this section, a controller based on the input-output feedback linearization theory, A. Isidori (1995), is defined for a MBC having an arbitrary number of levels  $N$ . This controller is derived by utilizing the reduced order model in (22). Employing the input-output feedback linearization technique, the following input can be considered

$$u_{av} = \frac{1}{L_g L_f^{r-1} h(x)} [-L_f^r h(x) + v]$$

Where  $r$  is the relative degree of the system, A. Isidori (1995), and it is obtained from

$$L_g L_f^{i-1} h(x) = 0; i = 1, 2, \dots, r - 1.$$

$$L_g L_f^{r-1} h(x) \neq 0$$

since

$$L_g h(x) = \frac{\partial h(x)}{\partial x} g(x) = [1 \ 0] \begin{bmatrix} \frac{x_2}{NL} \\ -\frac{x_1}{C(t)} \end{bmatrix} = \frac{x_2}{NL} \neq 0$$

system in (22) has a relative degree equal to 1 providing that  $x_2 \neq 0$ . Therefore, the input may be written as, A. Isidori (1995),

$$u_{av} = \frac{v - L_f h(x)}{L_g h(x)} \quad (23)$$

where

$$L_f h(x) = \frac{\partial h(x)}{\partial x} f(x) = -\frac{x_2}{NL} + \frac{E}{L}$$

$$L_g h(x) = \frac{\partial h(x)}{\partial x} g(x) = \frac{x_2}{NL}$$

By substituting the input (23) into (22), the state equation corresponding to the inductor current  $x_1$  is transformed into a linear form, this is

$$\frac{d}{dt} x_1 = v \quad (24)$$

In addition, parametric uncertainty will be addressed by using an integrator, this is

$$\frac{d}{dt} x_I = x_1 - i_{ref} \quad (25)$$

Then, a standard state feedback for the linear subsystem composed by (24)-(25) is defined as follow

$$v = -k_1 x_I - k_2 x_1 \quad (26)$$

In this particular case, the poles of the linear subsystem were proposed by considering a desired time constant for the closed loop system. The proposed poles are

$$s_{1,2} = [-1500 \ -1501]$$

Employing the pole placement technique, Hebertt Sira-Ramirez et al. (2006), the following gains are calculated

$$[k_1 \ k_2] = [2.2515 \times 10^6 \ 3001]$$

It is clear that the stability of the equilibrium point associated with the subsystem defined by (24) and (25) is guaranteed by selecting adequate gains of the standard linear state feedback in (26). On the other hand, the stability of the equilibrium point of the subsystem defined by the second state equation in (22) may be verified by analyzing the zero dynamics of that

subsystem, A. Isidori (1995). In order to analyze the zero dynamics, let us assume that  $v = 0$  and  $x_1(0) = i_{ref} = 0$ . Under these conditions, it is clear that  $x_1(t) = 0$  for all  $t$ . The input  $u_{av}$  can be rewritten now as

$$u_{av} = \frac{-L_f h(x)}{L_g h(x)} = \frac{\frac{x_2}{NL} - \frac{E}{L}}{\frac{x_2}{NL}} \quad (27)$$

Considering  $x_1(t) = 0$  and using (27), the second equation in (22) now becomes

$$\frac{d}{dt} x_2 = -\frac{N x_2}{RC(t)} \quad (28)$$

Let us consider the following Lyapunov function

$$V(x_2) = \frac{1}{2} x_2^2$$

its derivative is given by

$$\dot{V}(x_2) = x_2 \left[ -\frac{N x_2}{RC(t)} \right] = -\frac{N x_2^2}{RC(t)}$$

On the other hand, substituting  $C_{eq1}$  and  $C_{eq2}$  into the expression for  $C(t)$ , we obtain

$$C(t) = C u_{av} + C$$

From a practical standpoint, the duty cycle is defined in the range  $(0, 1)$ . This is  $0 < u_{av} < 1$ . Therefore  $C(t) > 0$ . Since parameters  $N$ ,  $R$  and  $C(t)$  are strictly positive, the derivative  $\dot{V}(x_2)$  is negative definite. Therefore the zero dynamics of the MBC is stable at  $x_2 = i_{ref}$ .

#### 4. Experimental results

As it was established earlier, the output voltage is indirectly controlled by defining a reference for the inductor current in terms of the desired output voltage. The expression that relates both variables is derived by carrying out a steady state analysis of the dynamic model in (22), i.e.

$$i_{ref} = \frac{V_{ref}^2}{RE} \quad (29)$$

where  $V_{ref}$  denotes the desired output voltage.

The implementation of the control law is carried out by employing RTAI-Lab, R. Bucher et al. (2008), as a Linux based real-time platform and a NI PCI-6024E data acquisition board. Fig. 9 depicts the Linux-based real time program of the implemented controller.

The parameters involved in the implementation are:  $L = 250 \mu H$ ,  $C = C_1 = C_2 = C_3 = 222.2 \mu F$ ,  $N = 2$ ,  $E = 30$  volts,  $R = 230 \Omega$  and  $V_{ref} = 150$  volts.

Figure 10 shows the experimental and simulated traces of the output voltage. It is important to note that since power losses in some electronic devices (diodes, transistor) are not included in the model defined by (22), the actual experimental measured output voltage is slightly smaller than the desired one.

Another experiment was designed for the purpose of showing a DC-DC multiplier boost converter in a wind energy generation system. Figure 11 shows the diagram of the wind energy conversion system. In this case, we consider a resistance as an electric load that is

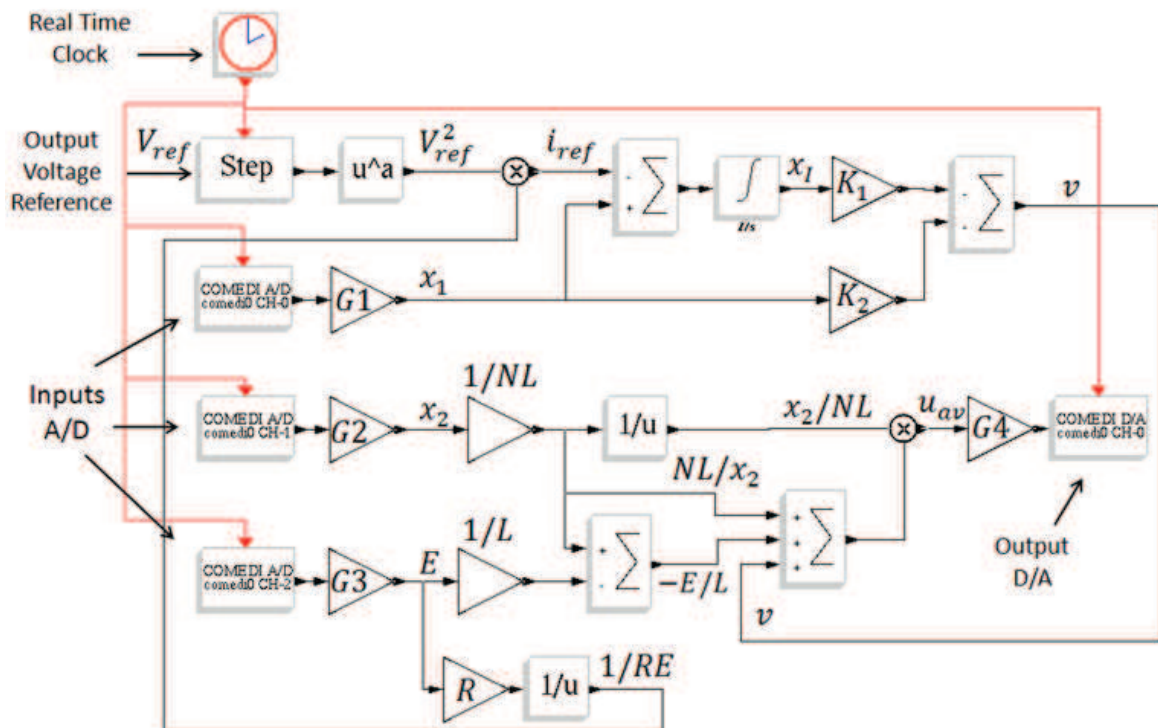


Fig. 9. Real time program of the implemented controller in RTAI-Lab.

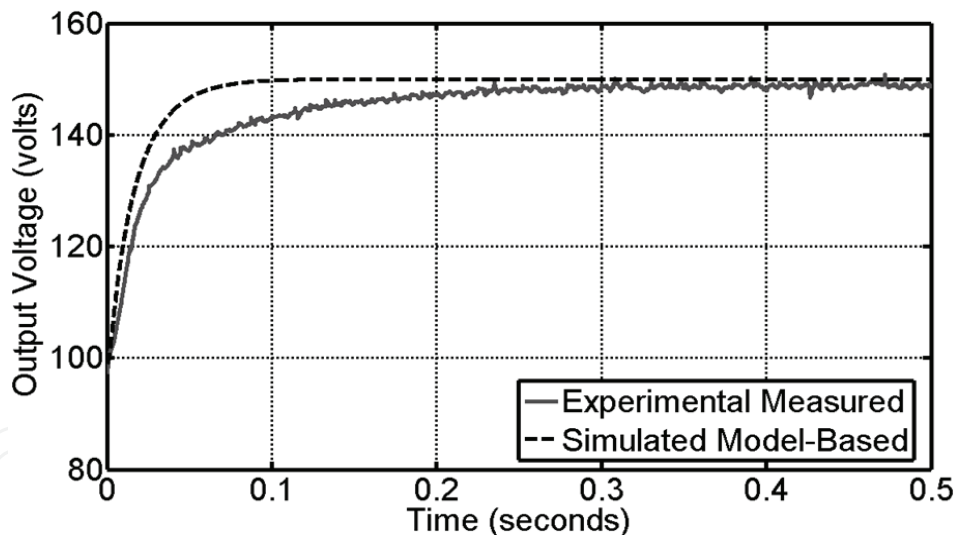


Fig. 10. Transient traces of the experimental measured and simulated model-based output voltage.

fed with a constant DC voltage. A variable speed wind turbine which is directly coupled to a permanent magnet synchronous generator is employed. As the wind speed changes, the generator speed changes as well. The result is a variable amplitude and variable frequency output voltage. In order to deal with this situation, the AC voltage is rectified by employing a standard uncontrolled AC-DC converter. Then, for the purpose of providing a constant DC voltage at the load terminals, a  $N \times$  MBC is included. It is important to note that this application works for a particular operation range. In other words, if the wind speed reaches very low or very high levels, the wind turbine may show an unstable behavior. In order to

avoid this situation, the electric load that is depicted in Fig. 11 may be replaced by a grid connected inverter. A feature of the grid connected inverter is that the energy extracted from the wind energy generation system can be defined depending on the wind speed.

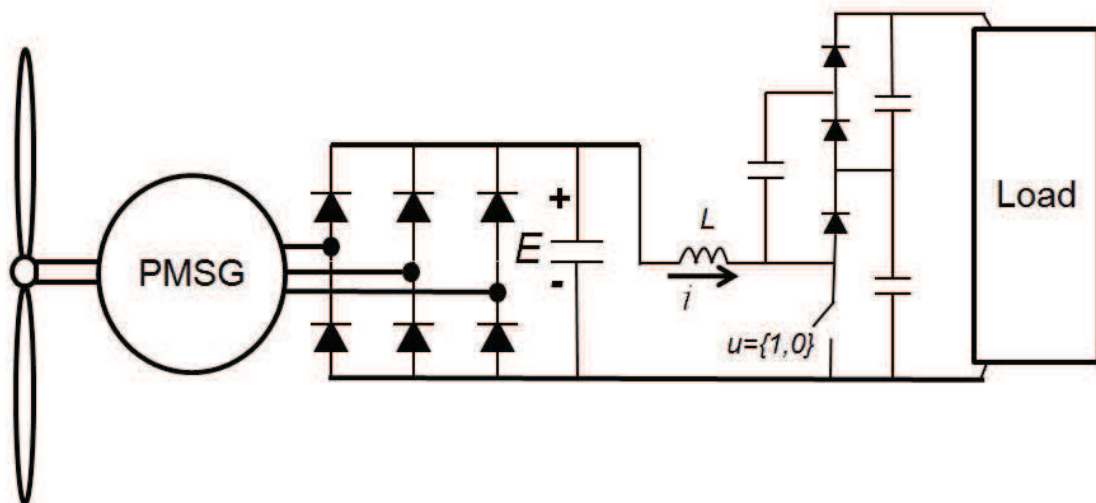


Fig. 11. Wind Energy Conversion System.

In the previous test the input voltage  $E$  is constant. In this new test, the input voltage  $E$  is varied as it is shown in Fig. 12. According to expression (29) the set point for the inductor current  $i_{ref}$  is calculated (in real time) as the input voltage  $E$  is varied. Figure 13 shows the experimental measured inductor current. The resulting experimental measured output voltage is depicted in Figure 14.

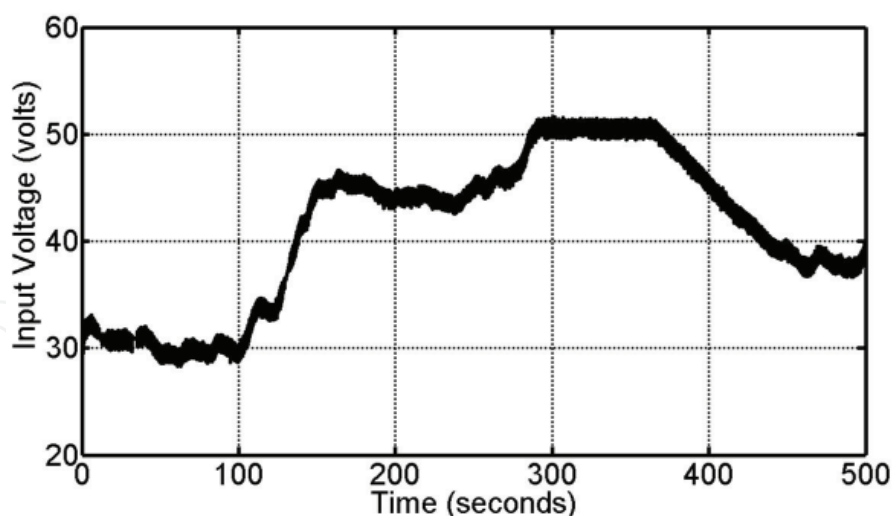


Fig. 12. Experimental input voltage  $E$ .

## 5. Conclusions

This work presents the state space modeling of a DC-DC Multiplier Boost Converter. Full and reduced order nonlinear models for the Nx MBC are proposed. A second order model is able to define an approximate dynamics for the Nx MBC having any number of levels. A

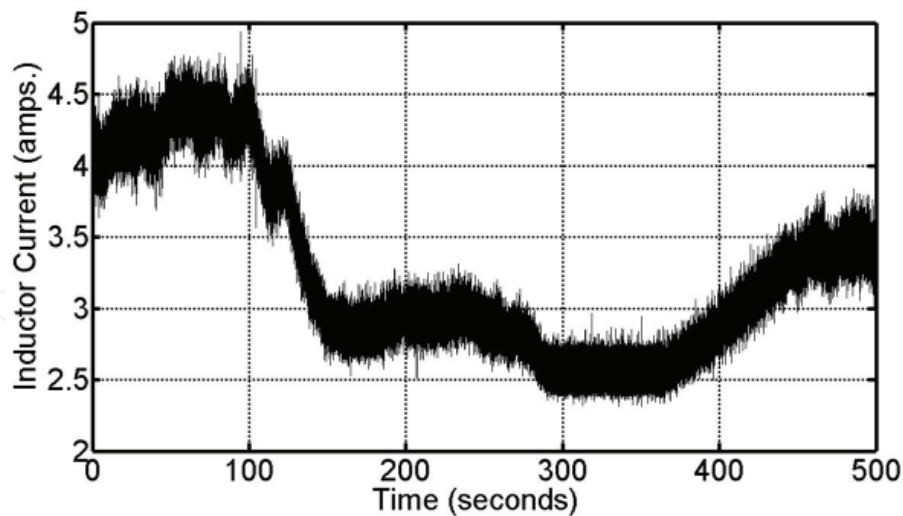


Fig. 13. Experimental inductor current when variations of the input voltage appear.

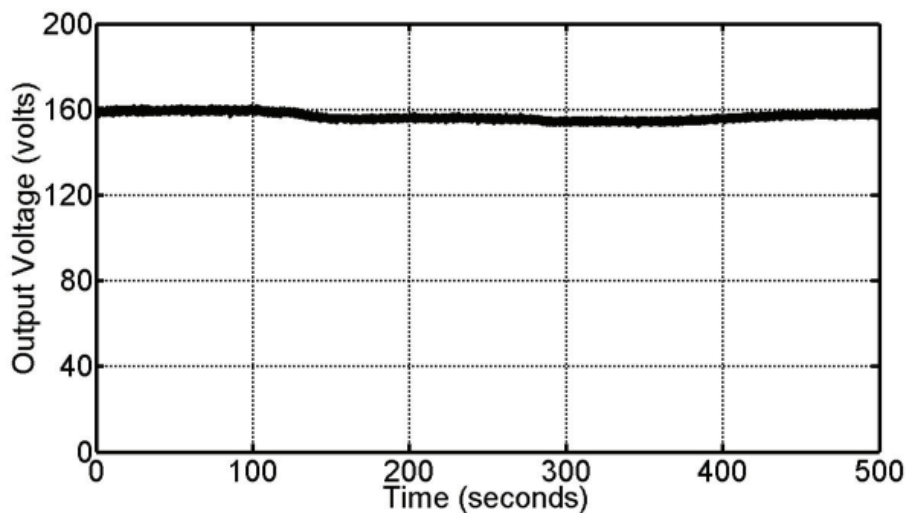


Fig. 14. Experimental measured output voltage when variations of the input voltage appear.

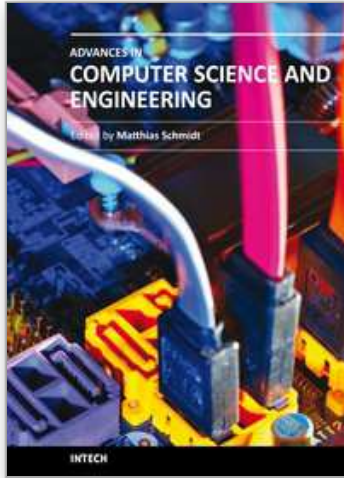
good agreement is obtained when comparing the full order and the reduced order models. In addition, the output voltage is indirectly controlled by using a control law based on the input-output feedback linearization technique. The controller is derived using the reduced order model of the  $N \times$  MBC. Excellent experimental results are shown for a  $2 \times$  MBC. In future works, a controller for the  $N \times$  MBC having higher number of levels will be implemented by using the reduced order model derived in this paper.

## 6. References

- R. D. Middlebrook, "Transformerless DC-to-DC converters with large conversion ratios". *IEEE Trans. Power Electronics*, vol. 3, Issue 4, pp. 484-488. Oct. 1988.
- D. Maksimovic; S. Cuk, "Switching converters with wide DC conversion range". *IEEE Trans. Power Electronics*, vol. 6, Issue 1, pp. 151-157. Jan. 1991.
- B. Axelrod; Y. Berkovich, A. Ioinovici, "Switched-Capacitor/Switched-Inductor Structures for Getting Transformerless Hybrid DC-DC PWM Converters". *IEEE Trans. Circuits and Systems I*, vol. 55, Issue 2, pp. 687-696, March 2008.

- Zhou Dongyan, A. Pietkiewicz, S. Cuk, "A three-switch high-voltage converter". *IEEE Transactions on Power Electronics*, Volume 14, Issue 1, pp. 177-183. Jan. 1999.
- Leyva-Ramos, J.; Ortiz-Lopez, M.G.; Diaz-Saldierna, L.H.; Morales-Saldana, J.A. "Switching regulator using a quadratic boost converter for wide DC conversion ratios". *IET Power Electronics*. vol. 2, Issue 5, pp. 605-613, Sept. 2009.
- Rosas-Caro, J.C.; Ramirez, J.M.; Peng, F.Z.; Valderrabano, A.; , "A DC-DC multilevel boost converter," *Power Electronics, IET*, vol.3, no.1, pp.129-137, Jan. 2010.
- Rosas-Caro, J.C.; Ramirez, J.M.; Garcia-Vite, P.M.; , "Novel DC-DC Multilevel Boost Converter," *Power Electronics Specialists Conference, 2008. PESC 2008. IEEE*, pp. 2146-2151, Jun. 2008.
- Rosas-Caro, J.C.; Ramirez, J.M.; Valderrabano, A.; , "Voltage balancing in DC/DC multilevel boost converters," *Power Symposium, 2008. NAPS '08. 40th North American*. Sept. 2008.
- Mayo-Maldonado J. C., Salas-Cabrera R., Cisneros-Villegas H., Gomez-Garcia M., Salas-Cabrera E. N., Castillo-Gutierrez R., Ruiz-Martinez O.; , "Modeling and Control of a DC-DC Multilevel Boost Converter," *Proceedings of the World Congress on Engineering and Computer Science 2010, Vol II, San Francisco, USA*. Oct. 2010.
- A. Isidori. *Nonlinear Control Systems*. Springer, 3rd edition, 1995.
- Morales-Saldana, J.A.; Galarza-Quirino, R.; Leyva-Ramos, J.; Carbajal-Gutierrez, E.E.; Ortiz-Lopez, M.G.; , "Multiloop controller design for a quadratic boost converter," *Electric Power Applications, IET* , vol.1, no.3, pp.362-367, May 2007.
- Bo Yin; Oruganti, R.; Panda, S.K.; Bhat, A.K.S.; , "A Simple Single-Input-Single-Output (SISO) Model for a Three-Phase PWM Rectifier," *Power Electronics, IEEE Transactions on*, vol.24, no.3, pp. 620-631, March 2009.
- Hebertt Sira-Ramirez and Ramon Silva-Ortigoza. "Control Design Techniques in Power Electronics Devices". Springer. 2006.
- Gensior, A.; Sira-Ramirez, H.; Rudolph, J.; Guldner, H.; , "On Some Nonlinear Current Controllers for Three-Phase Boost Rectifiers," *Industrial Electronics, IEEE Transactions on*, vol.56, no.2, pp. 360-370, Feb. 2009.
- R. Bucher, S. Mannori and T. Netter. RTAI-Lab tutorial: Scilab, Comedi and real-time control. 2008.

IntechOpen



## **Advances in Computer Science and Engineering**

Edited by Dr. Matthias Schmidt

ISBN 978-953-307-173-2

Hard cover, 462 pages

**Publisher** InTech

**Published online** 22, March, 2011

**Published in print edition** March, 2011

The book *Advances in Computer Science and Engineering* constitutes the revised selection of 23 chapters written by scientists and researchers from all over the world. The chapters cover topics in the scientific fields of Applied Computing Techniques, Innovations in Mechanical Engineering, Electrical Engineering and Applications and Advances in Applied Modeling.

### **How to reference**

In order to correctly reference this scholarly work, feel free to copy and paste the following:

J. C. Mayo-Maldonado, R. Salas-Cabrera, J. C. Rosas-Caro, H. Cisneros-Villegas, M. Gomez-Garcia, E. N. Salas-Cabrera, R. Castillo-Gutierrez and O. Ruiz-Martinez (2011). Dynamic Analysis of a DC-DC Multiplier Converter, *Advances in Computer Science and Engineering*, Dr. Matthias Schmidt (Ed.), ISBN: 978-953-307-173-2, InTech, Available from: <http://www.intechopen.com/books/advances-in-computer-science-and-engineering/dynamic-analysis-of-a-dc-dc-multiplier-converter>

**INTECH**  
open science | open minds

### **InTech Europe**

University Campus STeP Ri  
Slavka Krautzeka 83/A  
51000 Rijeka, Croatia  
Phone: +385 (51) 770 447  
Fax: +385 (51) 686 166  
[www.intechopen.com](http://www.intechopen.com)

### **InTech China**

Unit 405, Office Block, Hotel Equatorial Shanghai  
No.65, Yan An Road (West), Shanghai, 200040, China  
中国上海市延安西路65号上海国际贵都大饭店办公楼405单元  
Phone: +86-21-62489820  
Fax: +86-21-62489821

© 2011 The Author(s). Licensee IntechOpen. This chapter is distributed under the terms of the [Creative Commons Attribution-NonCommercial-ShareAlike-3.0 License](#), which permits use, distribution and reproduction for non-commercial purposes, provided the original is properly cited and derivative works building on this content are distributed under the same license.

IntechOpen

IntechOpen